Arabian Journal of Chemistry (2020) **13**, 7087–7103

King Saud University

Arabian Journal of Chemistry

www.ksu.edu.sa
www.sciencedirect.com

ORIGINAL ARTICLE

QbD-mediated RP-UPLC method development invoking an FMEA-based risk assessment to estimate nintedanib degradation products and their pathways

Balaji Jayagopal, Shivashankar Murugesh *

Department of Chemistry, School of Advanced Sciences, Vellore Institute of Technology University, Vellore 14, Tamil Nadu, India

Received 1 May 2020; revised 23 July 2020; accepted 23 July 2020
Available online 3 August 2020

KEYWORDS

QbD;
Analytical;
Degradation;
UHPLC;
MS;
Impurities

Abstract QbD is considered an important, fundamental, and integral part of dosage form development. Despite its significance in drug formulations, the knowledge, reference, and guidance for using QbD in analytical science have not been thoroughly documented in the literature. The present study is aimed at bridging the gap between its generated data and the unexplored terrain in formulation science. This study is novel because, for the first time, an exclusive shorter run time UHPLC method for estimating degradation products was developed through the QbD approach, validated, and proved stability indicative. Five degradation impurities were separated and well characterized. Further, the degradation pathway of the anticancer drug nintedanib (NIN) was explored for the first time in the soft gel formulation using tandem quadrupole MS abetted mass identification, and ESI/MS/MS aided structure elucidation was performed. By carefully demonstrating the step-by-step procedure for QbD-based optimization, parameters such as the analytical target profile (ATP) and critical quality attributes (CQAs) were assessed. The risk assessment was performed using failure mode effect analysis (FMEA). Critical method attributes and critical method parameters were identified based on the magnitude of the calculated risk priority number (RPN) value. Designed experiments using 4-factor two-level factorial design monitored three critical quality attributes to arrive at a method operable design space (MODS). The effect of individual method attributes was also analyzed using half-normal and Pareto charts. Control strategies design and RPN values were recalculated based on the DOE output. This RPN value is eventually identified to be significantly smaller and satisfactory within the allowable limit.

* Corresponding author.
E-mail address: mshivashankar@vit.ac.in (S. Murugesh).
Peer review under responsibility of King Saud University.

Production and hosting by Elsevier

https://doi.org/10.1016/j.arabjc.2020.07.014
1878-5352

1. Introduction

Idiopathic pulmonary fibrosis (IPF) is a progressive and eventually lethal lung disorder that leads to damage of lung function with deteriorating dyspnea and respiratory reflex (Keating, 2015). The occurrence of IPF in Europe and North America in the year 2000 was reported in nearly 6 people out of 0.1 million. Most studies showed an increase in occurrence over time (Hutchinson et al., 2015). Nintedanib binds competitively to the ATP binding pocket of fibroblast growth factor receptors, platelet-derived growth factor receptors, and vascular endothelial growth factor receptors and blocks the intracellular signaling that is crucial for the proliferation, migration, and transformation of fibroblasts representing the essential mechanism of action for IPF pathology (Mazzei et al., 2015).

The investigational drug is a salt form of nintedanib ethanesulfonate, which contains a carboxylic acid group linked to an indole ring. It is a chemically ethanesulfonic acid, namely, methyl 2-hydroxy-3-[N-[4-[methyl-[2-(4-methylpiperazin-1-yl)acetyl]amino]phenyl]-C-phenyl carbonimidoyl]-1H-indole-6-carboxylate, with a molecular weight of 649.76 g/mol and a base molecular weight of 539.62 g/mol (Togami et al., 2018). The ethane sulfonate salt is a bright yellow powder with pH-dependent solubility. The solubility increases at lower pH and decreases at higher pH. This result is largely due to the non-protonated free base, which is predominantly present as a nonpolarized moiety compared to the protonated form, which has a predominant salt structure.

Despite the continuous contributions from the pharmaceutical industry to new drug discoveries and innovations, poor manufacturing standards are a concern for the industry and the regulatory agencies. Hence, systematic approaches are mandated by the regulatory agencies and the manufacturers (Abboud and Hensley, 2003). Quality by design (QbD) is a systematic approach to new developments that begins with predefined objectives and emphasizes product and process understanding and process control based on sound science and quality risk management (ICH HARMONISED TRIPARTITE GUIDELINE, 2004). Although several guidelines and research articles for performing QbD-based formulation development have been published, a systematic understanding of analytical QbD and guidelines for its use are understandably scant. This work articulates the principles and practices of executing analytical QbD (AQbD) in quantitative systematic method development. In AQbD, the strategic purpose of the method and analytical target profile (ATP) are emphasized, while QbD addresses the outline quality target product profile (QTPP) (Jayagopal and Shivashankar, 2017).

Ultra-high-performance liquid chromatography (UHPLC) is a versatile purification technique that offers sub-2-mm particles with extended linear solvent velocities to provide dramatic improvements in resolution, sensitivity, and time of analysis. The reduced particle size to below 2 mm necessitates instrumentation for operating at pressures between 6000 and 15,000 psi. The characteristic peak width produced via UPLC is on the order of 1–2 s for a 10-min separation (Kochling et al., 2016).

UPLC coupled with a tandem quadrupole MS/MS detector is a new platform for producing molecular fragments useful for identifying degradant impurities by analyzing molecular fragmentation patterns. The present study used a scan wave enhanced product ion scanning mode provided by Waters Xevo TQS and a Micro Mass detector coupled with an Acquity UPLC-H Class. Mass Lynx V4.1 software enables a simpler check and confirms the structures of peaks of interest at a very low concentration. A standard T-wave collision cell was used simultaneously and confirms the superlative MRM quantification data and UPLC-MS/MS estimation with high speed and resolution (Plumb et al., 2004; Smith, 2018).

A forced degradation (FD) study is a necessary and integral part of drug development. A significant step in the drug development strategy is to provide valuable data on the shelf life of a drug in a shorter time (Görög and Baertschi, 2013). Mass spectrometry-mediated profiling of the forced degradation of drugs is a fairly new approach. Degradation pathways are elucidated based on a careful analysis of the fragmentation patterns of the $[M+H]^+$ ions of the main analyte and its degradants (Devrukhakar et al., 2017, 2018).

Several literature reports on NIN mainly focus on the protocol for estimating NIN in rat plasma (Togami et al., 2018). Further, NIN is used for the treatment of several diseases, including IPF, hypertension, and ovarian cancer (Tepede and Yogaratnam, 2017; Khalique and Banerjee, 2017). An assay procedure for estimating NIN has been documented with the specificity proved via forced degradation of samples (Dasari et al., 2015). Nevertheless, no literature report is available on the method development for estimating degradation products and explaining the mechanism of the degradation pathways of NIN. Furthermore, although a few literature reports suggested the QbD-based analytical test method for different classes of drugs, they did not offer sufficient information and clarity on predefining the CQA and ATP, risk assessment, identification of critical material attributes, critical method parameters and the complete QbD-based development flow (Karmarkar et al., 2011). An extensive literature search on NIN degraded study using QbD found no study reports on the proposal methodology. Therefore, we decided to assume the task of developing a systematic protocol development using mass spectrometry. A systematic approach to defining the flow of analytical method development through the QbD approach by predefining CQA (critical quality attributes) and ATP and conducting DOE by identifying critical material attributes and method parameters is reported in this study protocol. This work highlights the practice of failure mode effect analysis (FMEA) for the impartial identification of critical method parameters (CMPs) and critical material attributes (CMAs) associated with the resolution between closely eluted peaks. This approach will be used as an input for the DOE study of the optimization of method parameters (Mohammed et al., 2015). The present study is aimed at developing a novel stability indicating test method for quantifying the degradation products of NIN through a QbD approach, identifying, and characterizing the major degradation products formed, and suggesting the most likely degradation mechanistic pathways (see Scheme 1).

2. Experimental section

2.1. Chemicals

The NIN sample was provided by Solaris Pharm., India. Milli-Q water (filtered through a 0.22- μm membrane filter) was obtained from the Milli-Q high quality water system (Merck Millipore). Sodium hydroxide pellets, AR grade ammonium acetate, hydrochloric acid, gradient grade acetonitrile and hydrogen peroxide were purchased from Merck Millipore.

2.2. Instruments and data management systems

The separation analysis of NIN and its degradation products was achieved on an Acquity H-Class UPLC system (Waters, USA). The system was composed of H-class QSM solvent management pumps, an H-Class FTN sample manager, an Acquity PDA eλ detector, a solvent degasser and column compartment with a heater to control temperature. The data acquisition and processing were performed using Mass Lynx V4.1 software. All precision weighing was performed on a Mettler Toledo analytical balance (XPE 205, USA), and pH Seven Excellence (Mettler Toledo, USA) was used for pH measurements.

The Acquity UPLC is integrated with both a PDA detector to study the chromatographic pattern and a Xevo TQ-S micro-

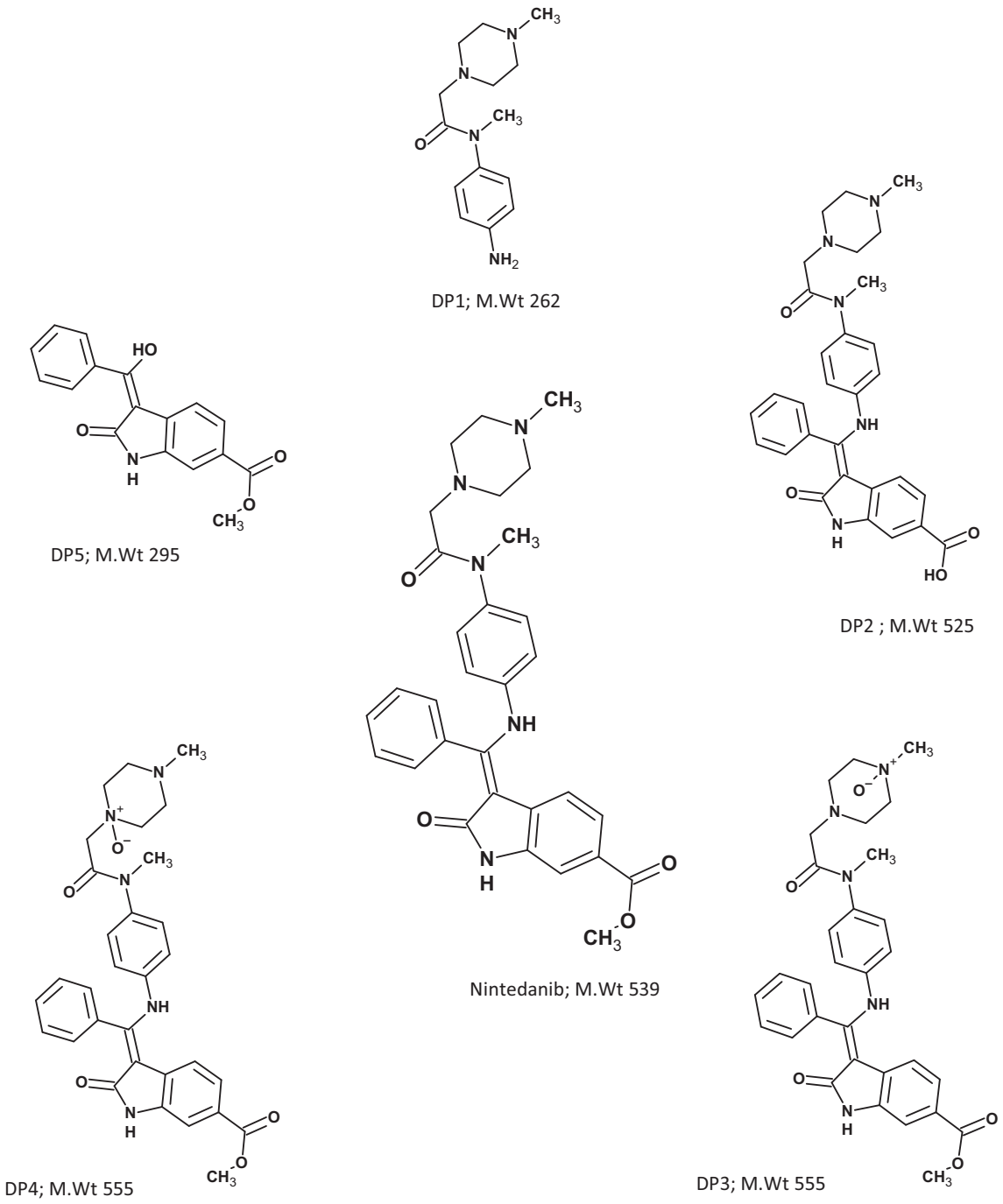

Scheme 1 Structure of NIN and proposed structures of its degradation products.

quadrupole mass spectrophotometer (Waters, USA) for mass analysis. The Xevo TQ-S micro-mass spectrophotometer is equipped with Z spray dual orthogonal API sources, step wave ion transfer optics, two high resolution and high stability quadrupole analyzers (MS1/MS2) with prefilters, and a T-wave enabled collision cell for optimal MS/MS performance. A photostability chamber (Newtronic, India) with UV and fluorescent lamps was used to perform the photodegradation procedure in compliance with the ICH guideline Q1B (ICH, 1998; Agency, 2011).

Design-expert Version 11.0 was used for designing experiments. Effect and interaction analyses were performed using a half-normal plot, Pareto chart, and 2D and 3D surface response plots.

2.3. Method development through QbD

2.3.1. Defining the quality (analytical) target profile

The systematic development of analytical method development starts by defining ATP. The ATP includes all attributes that

are needed to ensure the quality characteristics and purpose of the analytical method (Beg et al., 2015, 2016). Table 1 shows various elements of chromatography that are part of the target profiles for efficient method development.

2.3.2. Forced degradation and chromatographic conditions

To generate possible degradation products before separating and identifying the products, the drug was subjected to a forced degradation protocol. A 1 mg/mL solution of the drug in methanol underwent different chemical stress conditions: first, acid hydrolysis by treating it with 2 N hydrochloric acid followed by heating it at 80 °C for 1 h using a water bath; second, alkali hydrolysis with 0.2 N sodium hydroxide maintained at room temperature for 1 h; third, 3% hydrogen peroxide at room temperature for 4 h for oxidation, heating it at 80 °C in a water bath for 4 h for hydrolysis; fourth, photodegradation by exposing the drug molecule in solution to white florescence light of 1.2 million lux hours and UV light of 200-Watt h/m^2; and fifth, thermolytic degradation by exposing the solid material to 105 °C for 4 days in a hot air oven. A 5-µL aliquot of the degraded solutions was injected into an Acquity H Class UPLC system (Waters, USA) using the gradient elution mode of the Acquity UPLC HSS T3 column, a 0.005 M ammonium acetate buffer in pump A and acetonitrile in pump B. The flow rate, column temperature, and detector wavelength were set at 0.4 mL/min, 35 °C, and 250 nm, respectively.

Table 1 Analytical target profile and criticality.

ATP element	Target	Justification
Analyte	NIN and its degradation products	The degradation products of NIN shall be estimated
Sample	NIN soft gelatin capsules	Development of a method for the estimation of degradation products of NIN in NIN soft gelatin capsules.
Analytical technique	RP-HPLC/ RP-UPLC	RP-HPLC is a widely used analytical technique that facilitates a pierce separation of lipophilic substances (such as NIN, log Kow 1.89 [24] with a hydrophilic mobile phase and hydrophobic columns. High precision, quick analysis, low solvent consumption with small sample volume add additional advantages [25].
% RSD of Standard injection	Not more than 5.0%	Can be controlled by proper maintenance of chromatography and can be easily detected.
Resolution between any two impurities	Not less than 1.2	Affect quantification of impurities.
Recovery of impurities from the drug product	90.0–110.0%	Affect accuracy of impurities quantification.
Specificity	No interference due to blank and placebo, and separation between peaks	Affect quantification of impurities.
Linearity	Correlation coefficient (r): Not less than 0.99	The working concentration range will have absorbance less than 1.0 AU for a UV detector.
Precision	%RSD for replicate preparations should be not more than 5.0%	Affect quantification of impurities.
LOQ of impurities	Not less than 0.05%	Affects quantification of known and unknown impurities.

2.3.3. Identifying CQA

In formulation process development, CQA is generally identified from the manufacturing process parameters, whereas in AQbD analysis, outcomes such as resolution, accuracy of quantification, and peak shape are the possible CQAs (Yadav et al., 2015; Taylor et al., 2015). To identify the precise CQA, the sensitivity of the drug to various degradation conditions was studied. Five major degradants were identified from the degradation chromatograms. The resolution between a set of closely eluted peaks was considered for further risk assessment to evaluate the criticality. The acid, alkali and oxidative degradation sample chromatograms are presented in Fig. 1. The retention time (Rt) and relative retention time (RRT) of the peaks are listed in Table 2.

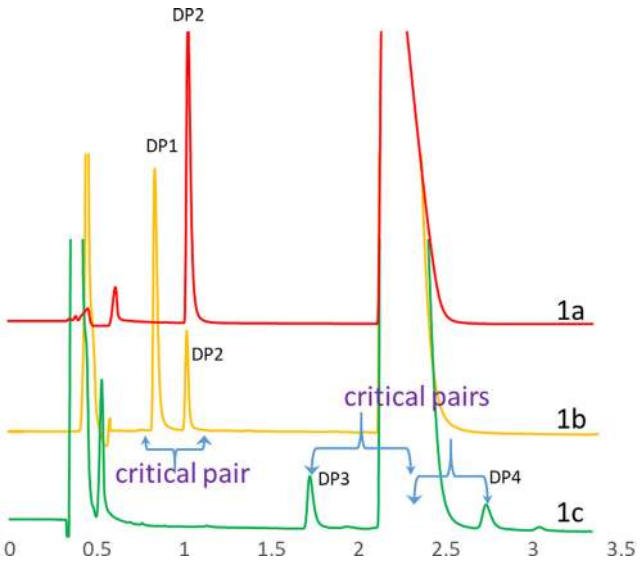

Fig. 1 a: Chromatogram of alkali hydrolysis sample with DP 2, b: Chromatogram of acid hydrolysis sample with DP 1 & DP 2, c: Chromatogram of oxidative degradation sample with DP 3 & DP 4. All chromatograms presented between 0 and 3.5 min for clear view while the actual run time is 12 min.

Table 2 Rt and RRt of nintedanib and its degradation products.

Peak	Rt (min)	RRT with reference to NIN
DP1	0.93	0.40
DP2	1.13	0.48
DP3	1.99	0.84
NIN	2.35	1.00
DP4	3.09	1.31
DP5	8.62	3.67

2.3.4. Risk assessment of the preliminary method

The CMPs that possess a high risk were identified through a risk assessment study based on their criticality and influence on CQAs. In addition, risk assessment also provides probable interaction(s) among the CMPs, assessing the probabilities of successive failure(s) (Basso et al., 2018). An Ishikawa fishbone diagram was sketched to determine the potential risks and corresponding roots that could affect the performance of an RP-HPLC method (Fig. 2) (Juran and Godfrey, 1998). The identified quality attributes of the method are subjected to an FMEA-based risk assessment. In the FMEA table, the impact of a failure to meet the quality attribute over the method objective is listed as a "potential impact" against the respective quality attribute. The method parameters (chromatography conditions) and material attributes (solvents and chemicals) that could potentially cause the failure are listed as a "potential cause". Further, the present control through system suitability procedures and other validation studies to detect failure are assessed as a "detection mode" in the FMEA table. The severity of the failure, chance of failure occurrence and detectability of failure were rated on a scale of 1 to 10 (1 = low, 10 = high). The risk priority number was calculated by multiplication of the values assigned for severity, occurrence, and detectability, where a higher RPN value indicates a worse criticality. The quality attributes were categorized as high or low critical based on the RPN value. The accomplishments of high risk CQAs were planned through DOE and those of the low risk CQAs, through a one-time validation study.

2.3.5. Identifying CMPs

All the chromatographic parameters, solvents and reagents used in the UPLC method are considered. Some of them are recognized as CMPs based on the criticality and knowledge acquired during primary method scouting. The bonded phase of the column was found to be CMP, but several columns of different bonded phases were evaluated during the preliminary method development, and only the superlative column was finalized at the end of scouting and considered for DOE.

2.3.6. Optimizing the effect of CMPs (method variables) on $CQA_{1\text{-}3}$ through DOE

A fractional factorial design was chosen over a full factorial design considering the number of factors (4) to be studied. The effects and interactions of critical method parameters ($CMPs_{1\text{-}4}$) identified through the risk assessment study were explored using a 2^n 4-factor regular two-level factorial experimental design with replication of the center point three times. A design matrix listing eight experimental measurements was generated using the design expert tool and executed by keeping other parameters, such as the wavelength, column, injection volume, buffer, sample concentration and diluent constant, at the desired value. Diluent, placebo, acid degradation, base degradation, and oxidative degradation samples were injected in each experimental condition. The acid degradation sample was neutral-

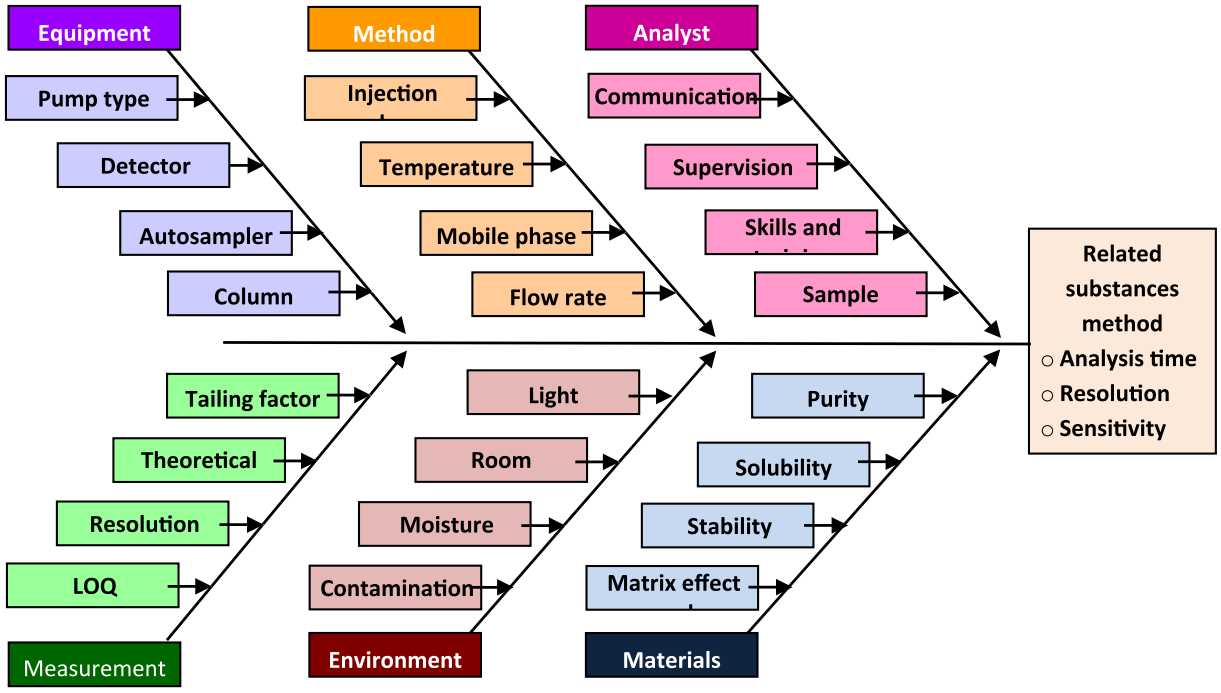

Fig. 2 Ishikawa diagram for risk identification and assessment.

ized with an equimolar concentration of sodium hydroxide. An excess amount of sodium hydroxide was added to the acid sample to generate a base degradation impurity to ease the calculation of resolution between the closely eluting peaks generated in acid and base degradation. The responses observed from the experiments were presented and analyzed using the polynomial 2FI mathematical model. Using a half-normal plot, variables and interactions with less significance were ignored during further modeling and ANOVA calculations. Effects and interactions were studied using Pareto charts and 3D and 2D contour plots. Further, the design space was established using an overlay plot. The polynomial equation was framed considering a model coefficient with a p value < 0.05. The suitability of the model was further backed by evaluating parameters such as the residual sum of squares and by performing a lack-of-fit analysis. Finally, the optimum condition was projected through numerical optimization and was marked using a flag in the overlay plot, which displays all the conditions within the desirability.

2.3.7. Diluent preparation

An aliquot of 100% methanol was injected as the diluent.

2.3.8. Placebo preparation

Approximately 80 mg of placebo (equivalent to 50 mg of NIN) was diluted with 50 mL of methanol and sonicated for 15 min.

2.3.9. Composite sample for acid and base degradation

Approximately 140 mg of capsule fill content (equivalent to 50 mg of NIN) was transferred to a 50-mL volumetric flask, 30 mL of methanol added, sonicated for 15 min, 5 mL of 5 N hydrochloric acid added, and heated at 80 °C for 1 h. The heating was followed by reflux condensation supplied with cold water to prevent methanol evaporation. The degraded solution was neutralized with 5.5 mL of 5 N sodium hydroxide, allowed to cool to room temperature, and made up to volume with methanol to obtain a 1 mg/mL solution.

2.3.10. Oxidative method of sample degradation

The sample was prepared by treating the drug with 3% hydrogen peroxide and allowing it to react at room temperature for 4 h. The final concentration of 1 mg/mL was prepared as mentioned above.

2.3.11. Validation studies

A 0.002 mg/mL solution of NIN was prepared in methanol and injected six times to evaluate the system precision. A concentration range of 0.0001–0.004 mg/mL of NIN was injected to establish a linearity that covers a working concentration of 0.01% to 0.04%. A minimum concentration with a signal- to-noise ratio above 10 was predicted as the quantification limit. A 0.0002 mg/mL solution was injected six times to check the precision at the LOQ level. Nintedanib was spiked at 0.0002, 0.001, 0.002 and 0.004 mg/mL to placebo to verify recovery of the drug in the presence of a placebo matrix. Six sample preparations, each a 1 mg/mL solution of NIN equivalent using the finished dosage form, were injected, and the % RSD of the %impurity was calculated to demonstrate the precision of the method.

2.3.12. Identification of impurities and elucidation of the degradation pathway

An enhanced tandem quadrupole mass spectrometric analysis (LC-ESI-MS/MS) was used to identify the mass and elucidate the structure of degraded structural units resulting from the forced degradation study. The integrated Acquity UPLC with both PDA detectors was used to study the chromatographic pattern, and a Xevo TQ-S micro-quadrupole mass spectrophotometer (Waters, USA) was used for mass analysis. The mobile phase carrying the components that flow out of the PDA detector was delivered into the mass spectrophotometer. The MS capillary voltage, cone voltage, MS mode collision energy, MS/MS mode collision energy, and scan time were set at 3.50 kV, 20.00 V, 3.00, 20.00, and 0.5 s in ES+ ionization mode, respectively. The selected daughter ions of the degradants were transferred to a quadrupole analyzer using collision induced disassociation (CID). A mass spectrogram was generated with the use of these detectors and was, in turn, used to propose a structure.

3. Results and discussion

3.1. Preliminary method scouting

NIN is a nonpolar molecule with a Log P value of 3.7 and poor water solubility. The dissociation constant of NIN was found to be 10.86 and 7.23 (Drug bank 5.1: Properties of Nintedanib). Considering the pKa, a mobile phase of pH 2.0 to 6.2 was preferred to avoid variation in retention time and poor peak shape due to ionization. Arriving at the basic chromatographic conditions highly depends on the physicochemical properties of the molecule. A good peak shape and adequate retention time and resolution depend on the column, pH and aqueous/organic concentration. Simultaneous method developments were performed using HPLC and UHPLC to separate the degradation peaks.

Columns of various bonding phases such as end-capped C18, polar group embedded C8, moderately hydrophilic octadecyl silica gel, and phenyl-hexyl bonded silica gel were screened, and the results are reported in Table 3. Among the bonded phases that were screened, the polar group embedded C8 column, namely, Symmetry Shield RP 8, was found to be more efficient in terms of resolution, peak symmetry, and peak height, possibly because of complimentary selectivity provided by the water layer at the pore surfaces and reduced undesirable secondary interactions between free and charged silanol groups.

Buffers with different pH levels were screened from 2.0 to 6.8. Because of uncharged silanol groups and cationic analytes obtained in the acid mobile phase, the peak symmetry, response, and separation at pH 2.2 were relatively better. Acetonitrile was chosen over methanol because, as an organic modifier, it efficiently eluted all the peaks with a better resolution and a shorter run time.

A minimum run time of 45 min was unavoidable, given the adequate chromatographic pattern with the Symmetry Shield RP 8 column, pH 2.2 perchlorate buffer, and acetonitrile as eluent. To minimize the run time, a change to the UPLC procedure was planned.

A stable bond C18 silica column, end-capped C18 column with a charged surface hybrid (CSH), end-capped C18 column

Table 3 Screening of organic modifiers.

Column	Organic Modifier	Bonded phase	Carbon (%)	Pore size (Å)	Plate count	Resolution			Tailing			Max response	Peak count
					Min	Min	Max	Mean	Min	Max	Mean		
X bridge Phenyl	ACN	Phenyl-Hexyl	15	130	5534	1.0	5.6	2.4	0.7	1.4	1.1	2,974,847	10
YMC pack ODS AQ	ACN	Moderately hydrophilic C18	14	120	3239	0.9	7.3	2.7	0.7	2.7	1.2	6,842,356	9
YMC pack pro	ACN	Endcapped C18	16	120	2466	1.1	10.9	2.3	0.8	1.6	1.0	3,413,493	15
Zorbax SB C18	ACN	Stable bond C18	10	80	4180	1.1	7.9	2.9	0.8	2.2	1.2	5,463,758	7
Symmetry Shiled RP8	ACN	Polar embedded C8 silica	15	100	3345Sc	1.1	13	2.4	0.8	1.6	1.0	3,401,439	16
Symmetry shield RP8	MeOH	Polar embedded C8 silica	15	100	5203	1.1	11.4	3.3	0.8	1.3	1.0	2,497,328	10
Symmetry shield RP8	MeOH: ACN (70:30)	Polar embedded C8 silica	15	100	2309	0.9	4.7	2.3	0.9	1.8	1.1	3,363,681	11

with an ethylene bridged hybrid (BEH) and end-capped C18 column with a high-strength silica were screened, and the observations are reported in Table 4. Because mass identification of the degradation products is part of the study plan, mass compatible buffers such as 0.001 M formic acid, 0.005 M ammonium formate, and 0.005 M ammonium acetate were screened. The combination of 0.005 M ammonium acetate buffer and an Acquity HSS T3 column with high-strength endcapped silica retained all interesting peaks with a minimum resolution of 1.2 in a dramatic 12-min run time. With acetonitrile in pump B contributing 40% of the initial gradient flow at a rate of 0.4 mL/min, the chromatography was considered satisfactory. The rapid resolution was supported using a column of smaller dimensions, namely, 100 mm (L), 2.1 mm (ID), and a 1.8 µ particle size. This preliminary method was considered for optimization through DOE.

3.2. Degradation behavior of NIN

Fig. 1 depicts UPLC chromatograms generated by injecting acid hydrolysis, alkali hydrolysis and oxidative degradation solutions. Two degradation impurities, DP1 and DP5, were generated under acid degradation conditions at a Rt of 0.93 and 8.62 min, respectively. A single major degradation impurity (DP2) was formed under alkali degradation at a Rt of approximately 1.1 min, and two degradation products (DP3 and DP4) were observed in the oxidative degradation chromatogram at a Rt of approximately 1.99 and 3.09 min. As summarized in Table 5, the drug molecule was found to be more sensitive for alkali concentrations. Even at a lower alkali concentration, the drug molecule was found to degrade 70–80% of NIN and was moderately sensitive to acidic and oxidative degradation. The water hydrolysis sample showed no degradants, indicating that the drug was quite stable under neutral stress conditions. No degradation products were observed during photolysis and thermolysis.

3.3. Risk assessment studies

From the degradation chromatograms and the Rt and RRT of the analyte, it is evident that peaks {DP1, DP2}, {DP3, NIN} and {NIN, DP4} elute closely and that all three separations are sensitive and further considered as critical quality attributes (henceforth denoted CQA_1, CQA_2 and CQA_3, respectively). Table 6 illustrates the FMEA hypothesis for identifying risks associated with each CQA. The study suggests that all three resolutions have a high RPN value, and the method parameters that could act as a potential cause of the failure were identified as CMPs. Table 7 shows that the flow rate, column temperature, organic ratio and gradient program are considered CMPs to achieve the target profile and are denoted CMP_1, CMP_2, CMP_3, and CMP_4, respectively. The other CQAs, such as the LOQ precision, recovery, and specificity, are denoted $CQA_{4\text{-}6}$, respectively. Table 8 shows the accomplishment plan for decreasing the high RPN value as calculated in the FMEA hypothesis. $CMP_{1\text{-}4}$, which are identified as potential causes of the failure of $CQA_{1\text{-}3}$, underwent a DOE study, and the accomplishment plan for $CQA_{4\text{-}6}$ was obtained through validation studies.

Table 4 Screening of UPLC columns.

Mobile phase buffer	Rt (min)					Minimum resolution between peaks	Inference
	DP1	DP2	DP3	NIN	DP3		
Acquity C18 BEH	0.40	0.47	0.56	0.75	0.81	0.90	DP1 merged with diluent peak and DP4 merged with NIN peak
Acquity C18 CSH	1.27	1.55	2.01	2.71	3.20	0.95	DP1 merged with diluent peak
Acquity C18 HSS T3	1.16	1.41	1.83	3.00	3.93	1.20	Peaks are well separated

Table 5 Forced degradation study.

Stress condition	Treatment	No. of degradation products (Rt in mins)	Total degradation (%)	Assay (%)
Control sample	No treatment	–	–	100.8
Acid degradation	2 M HCl heated at 80 °C, 1 h	2 (0.93 & 8.82)	1.2	98.9
Alkali degradation	0.2 N NaOH, 1 h	1 (1.13)	3.0	96.1
Oxidation	3% H_2O_2, 4 h	2 (1.99 & 3.09)	0.5	100.2
Thermal degradation	100 °C, 4 days	–	–	99.9
Hydrolysis	Water at 80 °C, 4 h	–	–	99.5
Photodegradation	White florescence light of 1.2 million lux hours & UV of 200-Watt h/m^2	–	–	100.5

Table 6 FMEA for identification of CMPs for related substances method.

Quality attributes	Type of risk/failure	Potential Impact	SEV	Potential Causes	OCC	Detection Mode	DET	RPN
Specificity	Interference due to diluent peaks at Rt of impurities	Inaccurate quantification of impurities (due to merging)	3	Poor quality of reagents & solvents	3	chromatogram review	2	12
Specificity	Placebo interference (Specificity)		3	Organic concentration, flow rate, column temperature, gradient program (CMA)	3		2	12
DP1 & DP2 quantification	Merging of DP1 & DP2		3		3		3	27
DP3 quantification	Merging of DP3 & main analyte	The presence of impurity may be completely unknown	3		3		3	27
DP4 quantification	Merging of main analyte & DP4		3		3		3	27
LOQ of impurities	Poor response	Poor quantification	2	Sample concentration & analytical technique	2	Signal to Noise ratio	3	12
Recovery	Could be less than 80%	Inaccurate quantification	2	Poor solubility of impurities in diluent	2	Recovery study	3	12

SEV- severity (1 = low, 4 = high); OCC– occurrence (1 = low, 4 = high); DET- detectability (1 = low, 4 = high).
RPN -risk priority number (RPN = SEV × OCC × DET).

Table 7 Listing of critical method and material attributes and their impact on CQAs.

Material attributes & Method parameters	Is parameter critical for CQA? (Yes/No)				Observation
	CQA1	CQA2	CQA3	CQA4	
Flow rate	Yes	Yes	Yes	Yes	Flow rate can alter the elution time
Injection volume	No	No	No	No	No impact on resolution
Organic concentration	Yes	Yes	Yes	Yes	Can change the elution pattern
Gradient program	Yes	Yes	Yes	Yes	Can change the elution pattern
Detection wavelength	No	No	No	No	No influence in chromatographic pattern
Column temperature	Yes	Yes	Yes	Yes	Can alter the separation between peaks
Buffer pH	No	No	No	No	No impact observed for this molecule
Column	Yes	Yes	Yes	Yes	Can alter the separation and elution pattern.
Sample temperature	No	No	No	No	No influence on separation and elution order.
Grade of acetonitrile	No	No	No	No	No interference due to diluent observed
Grade of ammonium acetate	No	No	No	No	No interference due to diluent observed

Table 8 Accomplishment plan based on RPN and ATP criteria.

CQA	ATP	RPN	RPN remark	Accomplishment plan
Minimum resolution between DP1 & DP2 (CQA1)	Not less than 1.2	27	High	DoE with respective CMPs
Minimum resolution between DP3 & main analyte (CQA2)	Not less than 1.2	27	High	DoE with respective CMPs
Minimum resolution between main analyte & DP4 (CQA3)	Not less than 1.2	27	High	DoE with respective CMPs
LOQ Concentration (CQA4)	Less than 0.05%	9	Medium	Through validation and control strategy
Recovery (CQA5)	90.0–110.0%	9	Medium	Through validation and control strategy
Specificity (CQA6) Blank & placebo interference	No Interference at analyte Rt	9	Medium	Through validation and control strategy

Table 9 Range of four CMPs considered for DoE.

Symbol	Chromatographic variables	Low	High
A	Flow (mL/min) (CMP1)	0.35	0.45
B	Column temperature (°C) (CMP2)	35.0	45.0
C	Organic concentration (%) (CMP3)	35.0	45.0
D	Gradient increment (Gradient rate) (CMP4)	0.70	1.30

3.4. Analysis of DOE results for various critical method parameters (CMPs)

The −1 and +1 values for all four CMPs considered for DOE are presented in Table 9. $CQA_{1\text{-}3}$ are monitored as responses for the DOE experiment, and they are denoted R1, R2, and R3, respectively. The DOE matrix and the responses are listed in Table 10. Figs. 3 and 4 depict the half-normal plots and Pareto charts illustrating the influence of CMAs on responses R1-3. The Pareto-ranking analysis showed that the impact of factors (i.e., column temperature, flow rate, organic concentration, gradient flow rate) on the CQAs was statistically significant ($P < 0.05$), and thus, the factors were designated as the CMPs for further optimization studies (see (see Table 12).

The interpretation of the effect of each CMP on the resolutions based on the DOE results is presented in Table 11.

The half-normal plot and the Pareto chart show that the column temperature has a substantial influence on all three peak resolutions R1, R2 and R3 ($CQA_{1\text{-}3}$). An increase in the temperature of the chromatographic bed reduces the viscosity of the mobile phase and improves the diffusion. Considering the thermodynamic rule of reversed-phase chromatography, an increase in temperature expedites the component elution and consecutively coelutes peaks, thus decreasing the resolution.

The organic concentration is inversely proportional to the resolutions R1, R2 and R3. Acetonitrile, known for its elution strength, expedites the elution of hydrophobic compounds and thus reduces the peak spacing.

The gradient increment rate (organic flow rate) is directly proportional to R1 and R2 (CQA_2) and inversely proportional to R3. The varying composition of the mobile phase and the difference in affinities between the two components causes the varied resolutions.

The flow rate and column temperature have a synergic, positive effect in maximizing R2 (CQA_2). An increased linear velocity and increased diffusion resulted in narrow peaks with increased resolution.

The model analysis results are presented in Table 12. The model F-value implies that the model is significant. P-values < 0.0500 indicate that the model terms are significant. The lack-of-fit F-value implies that it is not significant relative to the pure error. A non-significant lack of fit is good with an expectation of the model to be fit.

Table 10 DOE matrix for 4 factor 2 level factorial design and response data.

Std	Run	CMP1	CMP2	CMP3	CMP4	R1	R2	R3
5	2	0.35	35	45	1.3	1.39	1.68	1.27
1	5	0.35	35	35	0.7	1.47	1.82	2.46
7	6	0.35	45	45	0.7	0.47	1.07	1.18
3	11	0.35	45	35	1.3	0.51	1.35	1.13
11	7	0.4	40	40	1	0.79	1.45	1.43
10	8	0.4	40	40	1	0.75	1.46	1.60
9	10	0.4	40	40	1	0.94	1.55	1.60
4	1	0.45	45	35	0.7	0.6	1.38	1.68
6	3	0.45	35	45	0.7	1.29	1.5	2.41
8	4	0.45	45	45	1.3	0.55	1.35	1.11
2	9	0.45	35	35	1.3	1.45	1.74	2.31

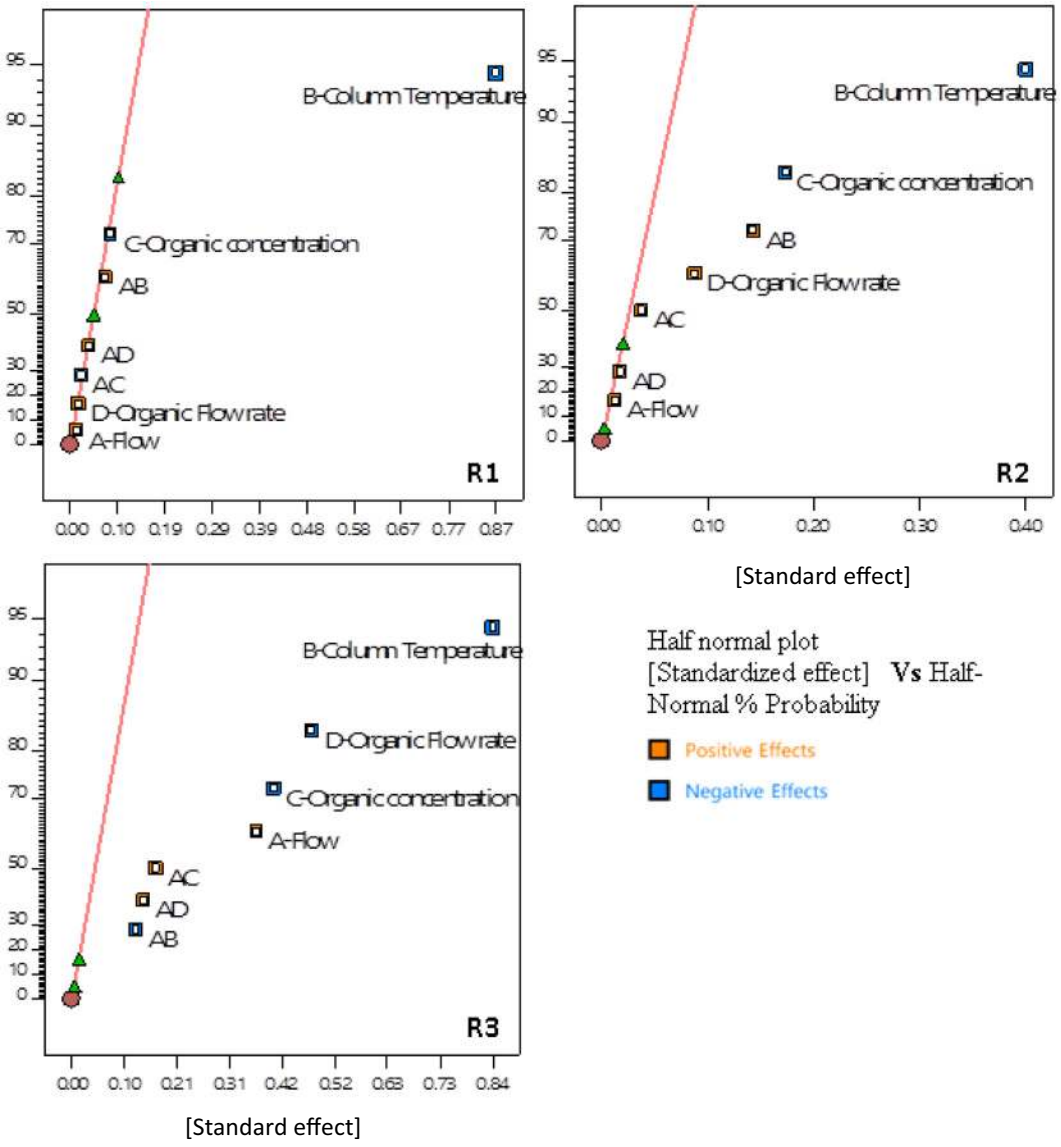

Fig. 3 Effect analysis by half normal plots.

Further, the response surface mapping was performed with the help of the 3D response surface and 2D contour plots for each CQA (responses), as shown in Fig. 5. The 2D plot for response 1 reveals that decreases in the column temperature and flow rate maximize the peak resolution R1 (Fig. 5A) and R2 (Fig. 5E). In contrast, an increase in flow rate and a decrease in column temperature and organic concentration increase the peak resolution R3 (Fig. 5B and 5C). The organic concentration and gradient increment rate have no significant influence over peak resolutions R1 and R2, whereas an increase in the organic concentration has a negative effect on peak resolution R2 (Fig. 5F). The desirability plot (Fig. 5G) shows that the flow rate and column temperature should be kept at the minimum to obtain a peak resolution within the desired range.

The final equation in terms of coded factors generated using statistical analysis of response establishes the relation between CMPs and CQAs (Table 13). The equation is used to make predictions about the response for given levels of each factor. Further, the coded equation is useful for identifying the relative impact of the factors by comparing the factor coefficients. The compilation of calculated responses and the mean response of three determinations that were performed by following the parameters (solution with high desirability value) suggested by the design tool and the mean responses of the three determinations are comparable to the calculated results.

3.5. Defining the design space

Finally, a design space was created by defining the desirability for all three CQAs involved in the related substances method. Apart from the interesting CMPs, the remaining chromatographic parameters that were not critical were held constant at the desired level as finalized in the initial method develop-

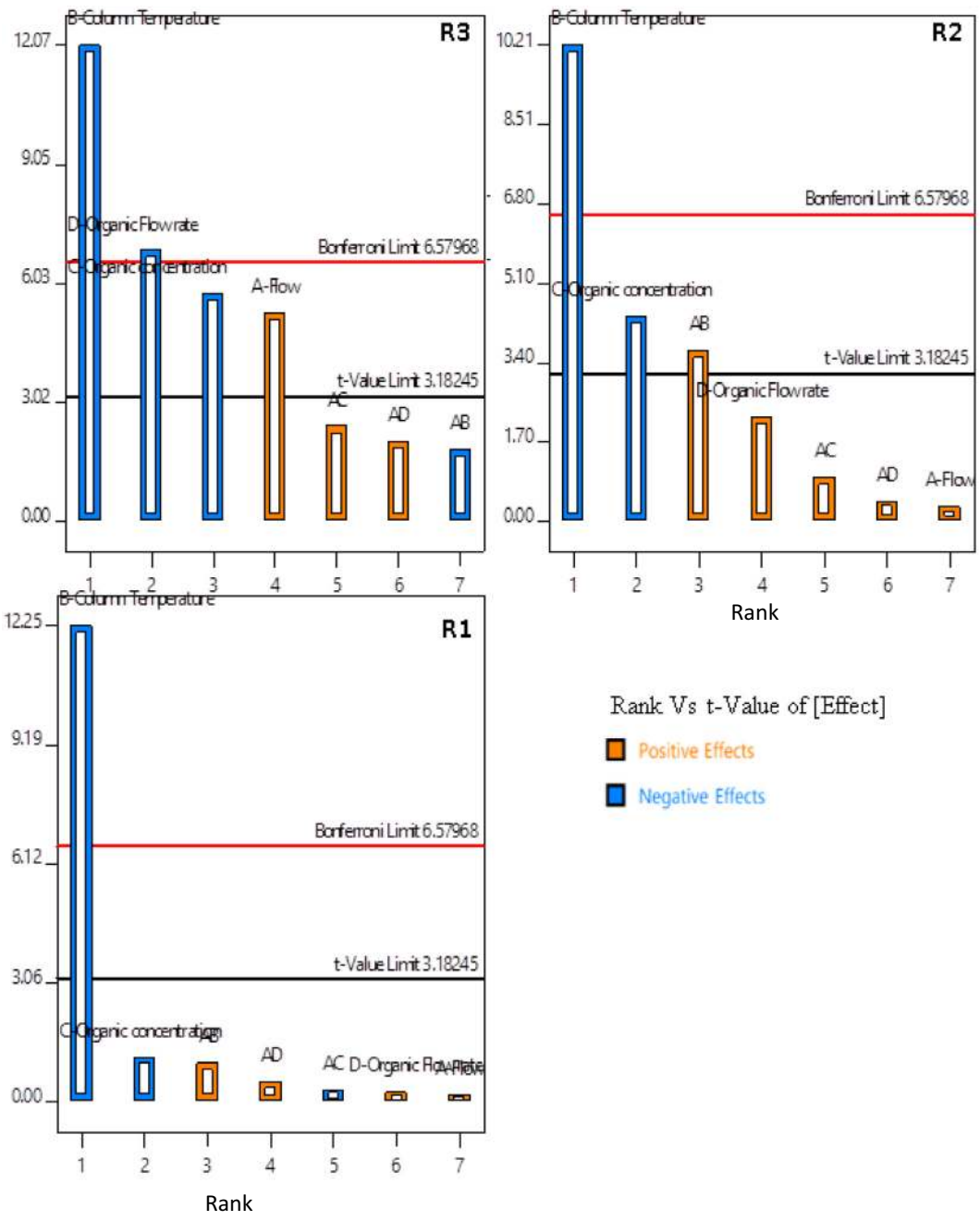

Fig. 4 Pareto charts showing individual factor effects and combination effects.

ment and mentioned in the FMEA. An overlay plot drawing a space within which CMPs could be changed without affecting CQAs was generated for all the CMPs. The desirability was set to maximize the resolution with a minimum resolution of 1.2 for all three separations. This agreeable region is the confirmed acceptable range (yellow region, Fig. 6) within which the method variation meets the desirability. The optimum condition is marked with a flag in the overlay plot that displays all the conditions. The flagged conditions were a column temperature of 35 °C, flow of 0.4 mL/min, organic concentration of 35.0% and gradient increment rate of 1% per min. These conditions were further considered for validation with the gradient program (refer supplementary document)

3.6. Defining control strategies for all CQAs and CMPs

Eventually, the control strategy for the four CMPs was drawn from the DOE study, and the result is presented in Table 15. These CMPs and CMAs are kept under control and monitored closely during routine usage at the quality control laboratory.

3.7. FMEA: Risk assessment moderation

Assessing the effect of DOE on the RPN and correlating it with the values observed before performing DOE is the concluding step, i.e., with FMEA, the RPN values decreased

Table 11 Summary of effect and interaction analysis.

Critical Method parameters	CQAs		
	R1	R2	R3
Flow rate (A)	∝	∝	∝
Column temperature (B)	1/∝	1/∝	1/∝
organic concentration (C)	1/∝	1/∝	1/∝
Gradient program (D)	∝	∝	1/∝
AB	∝	∝	1/∝
AC	1/∝	∝	∝
AD	∝	∝	∝

∝	Proportional to the change		High
			Moderate
			Low
1/∝	Inversely proportional to change		High
			Moderate
			Low

significantly for the CMPs in Table 14 (compare with the RPN values in Table 8).

3.8. Validation results

The method was linear from 0.0001 mg/mL to 0.01 mg/mL with an acceptable regression coefficient (r^2) value of 0.998. The predicted LOQ and LOD for NIN were 0.002 and 0.00006 mg/mL, respectively. The RSD values for the method precision, injector precision and LOQ precision were 2.6%, 1.4% and 4.5%, respectively. The recovery results calculated from the "mg added" and "mg found" were between 96.1 and 104.6% for NIN in the concentration range of LOQ to 0.0004 mg/mL, Table 15 presents the individual recovery values and the inter-day and intraday precision results.

3.9. Identification and interpretation of MS/MS fragments of degradation products

3.9.1. MS/MS CID of degradation products

The selected daughter ions of degradants were transferred to the quadrupole analyzer using collision induced disassociation (CID). A mass spectrogram was generated using these detectors that, in turn, was used to propose the structure (Schemes S1-4). A list of daughter ions obtained for each degradant product is provided in Table 16. The observed m/z is comparable with the calculated m/z (Table 17).

3.9.2. Interpretation of fragments

The ESI positive mass spectrum of the NIN peak shows a [M + H] + ion with m/z 540. Fragment ions at m/z 412 (loss of $C_6H_{12}N_2O$), m/z 399 (loss of CH from m/z 412), m/z 294 (loss of C_7H_7N from m/z 399), m/z 249 (protonated N-(4-aminophenyl)-N-methyl-2-(4-methylpiperazin-1-yl) acetamide), and m/z 219 (N-phenyl-2-(piperazine-1-yl) acetamide) were observed in the MS/MS spectrum (refer supplementary document).

3.9.3. DP1 and DP5 ([M+H]+, m/z 263 and m/z 296)

By injecting the acid catalyzed degraded sample, a major degradant was observed at retention times of 0.90 and 8.6 min, labeled DP1 and DP5, respectively. The ESI-MS/MS spectrum of m/z of 263 (DP1) shows product ions at m/z 151 (protonated N-(4-aminophenyl)-N-methylformamide from loss of 1,4-dimethyl piperazine), m/z 113 (1,4-dimethyl piperazine), and m/z 136 (protonated dimethyl-p-phenylenediamine, loss of oxygen from m/z 151) (refer supplementary document). The fragments m/z 151 and 113 are evidence of the proposed mechanism of hydrolysis at the secondary amine reactive center, resulting in the formation of amine DP1 (amine) and DP5 (alcohol), as mentioned in Scheme 2. These MS/MS data indicate that DP1 is N-(4-aminophenyl)-N-methyl-2-(4-methylpiperazin-1-yl) acetamide.

The ESI/MS/MS spectrum of m/z 296 (DP5) shows product ions at m/z 219 (loss of C_6H_6, OH) and m/z 190 (loss of CH_2 from m/z 219). From the m/z fragments, it is understood that DP1 and DP5 are products of the same acid hydrolysis reaction at the secondary amine of NIN at position 19. These MS/MS data lead to the conclusion that DP5 is (3Z)-3-[hydroxy(phenyl)methylidene]-2-oxo-1H-indole-6-carboxylate (refer supplementary document).

3.9.4. DP2 ([M+H]+, m/z 526)

The chromatogram of the base hydrolysis sample shows a major degradation peak at a retention time of 0.97 min, labeled DP2. DP2 has a m/z of 526 from demethylation of NIN. The product ions at m/z 398 (loss of $C_6H_{12}N_2O$), m/z 385 (loss of CH from m/z 398), and m/z 249 (protonated N-(4-aminophenyl)-N-methyl-2-(4-methylpiperazin-1-yl) acetamide) were observed in the ESI/MS/MS spectrum of [M+H]+ ions (m/z 526) (refer supplementary document). The absence of fragment m/z 412 when compared to Nin fragmentation and the formation of fragment ion m/z 398 indicate the presence of a methyl group at positions 11 and 10, illustrating that demethylation occurred at position 39. These MS/MS data lead to the conclusion that desmethyl NIN is (3Z)-3-[({4-

Table 12 ANOVA table.

Source	Sum of Squares	p-value	Sum of Squares	p-value	Sum of Squares	p-value	Inference
	CQA_1		CQA_2		CQA_3		
Model	1.57	0.0001	0.4352	0.0086	2.59	0.0416	Significant
Residual	0.0220		0.0061		0.1092		
Lack of Fit	0.0019	0.9739	3.788E-07	0.9921	0.0547	0.2921	Not significant
Pure Error	0.0201		0.0061		0.0545		

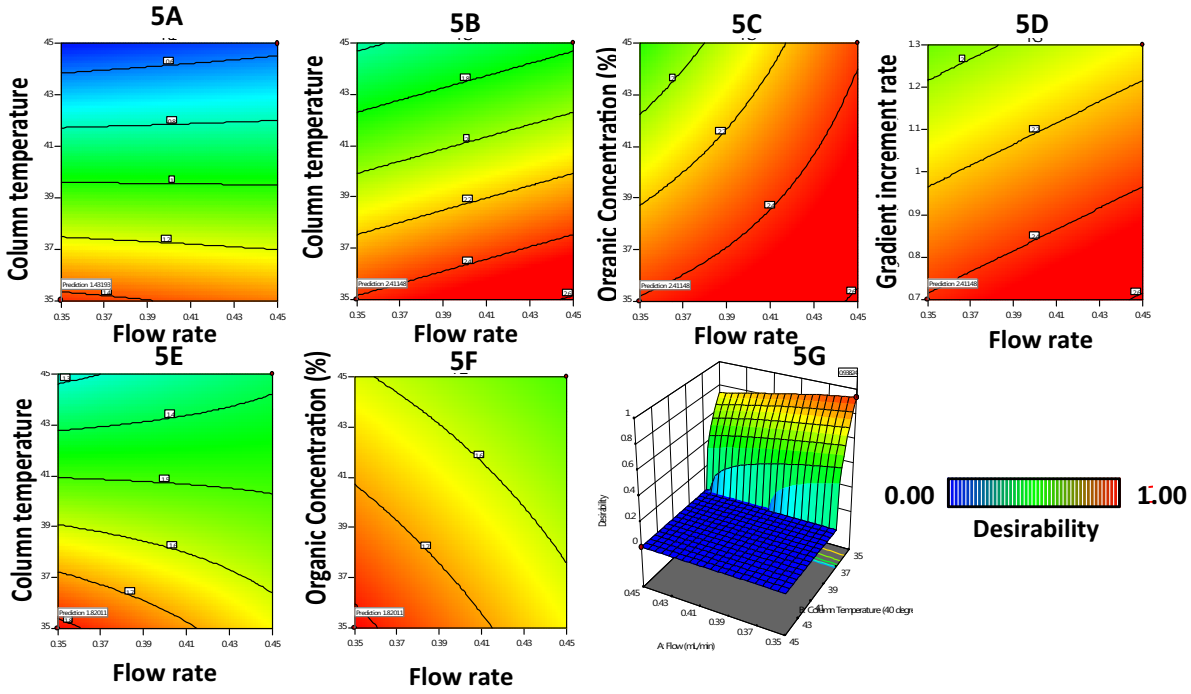

5A - illustrates response R1, 5E & 5F- Illustrates response R2 and 5B, 5C & 5D – illustrates response R3.

Constant conditions: column temperature 35°C, organic concentration 40%, flow rate 0.4 mL, gradient rate increment 1%.

Fig. 5 **A–G** 2D plots of CMAs, namely (A–F) and G desirability plot.

Table 13 Final equations in terms of coded factors.

Response	Polynomial equation
R1	RS1 = 0.8267–0.4338B – 0.0412C + 0.0362 AB + 0.0187AD + BC + CD + 0.1396 ABCD
R2	RS2 = 1.49 + 0.0063A – 0.1988B – 0.0862C + 0.0438D + 0.0712AB + 0.0187AC + 0.0088AD + BC + BD + CD
R3	RS3 = 11.82–13.15A – 0.294B + 0.1175C – 2.556D + 0.48AB – 0.36AC + 7.0 AD

[N-methyl-2-(4-methylpiperazin-1-yl) acetamido] phenyl} amino) (phenyl)methylidene]-2-oxo-1H-indole-6-carboxylic acid.

3.9.5. DP3 ([M + H] +, m/z 556), DP4 ([M + H] +, m/z 556)

The chromatogram oxidative degradation sample shows major degradation peaks at 2.39 min and 3.09 min, which are denoted DP3 and DP4, respectively. Product ions at *m/z* 412 (loss of ($C_6H_{12}N_2O_2$), *m/z* 399 (loss of CH from *m/z* 412), *m/z* 294 (loss of C_7H_9N from *m/z* 399), and *m/z* 219 (loss of methyl (3Z)-3-[amino(phenyl)methylidene]-2-oxo-1H-indole-6 -carboxylate and piperazine ring opening at position 2) were observed in the ESI/MS/MS spectrum of [M + H]+ ions (*m/z* 556, DP3) (refer supplementary document). The fragment

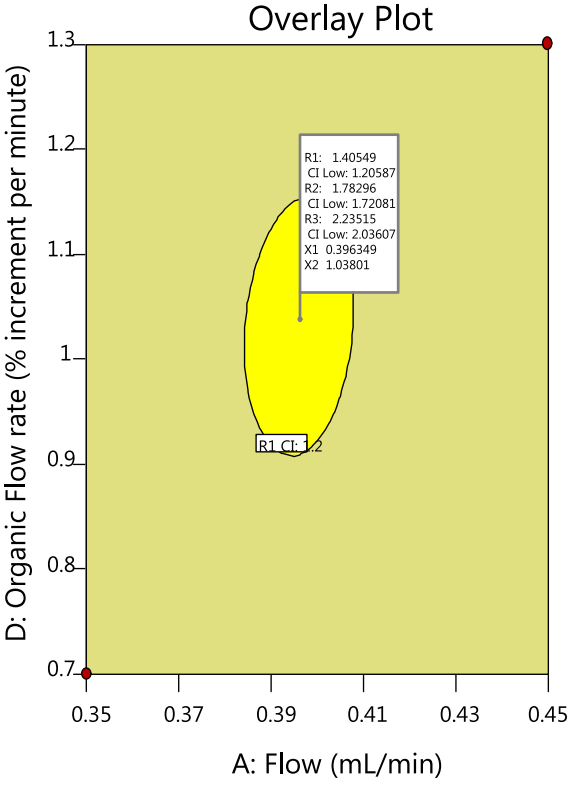

Fig. 6 Design space with column temperature at 35 °C and organic concentration 35%.

Table 14 Revised RPN after FMEA with the control strategy for the CMPs.

Failure Type	Recommended Actions	Control strategy	SEV	OCC	DET	RPN	% decrease in RPN
Interference due to diluent peaks at Rt of impurities	Defining chromatography grade of solvents & reagents in methodology. Inclusion of diluent injection in the sequence.	Reagents and solvents grade evaluated and mentioned in the procedure. Diluent injection recommended in the injection sequence of test procedure.	3	1	1	3	75
Placebo interference	Overlay the placebo chromatogram with sample chromatogram and evaluate.	Placebo included in the procedure to compare	3	1	1	3	75
Merging of DP1 & DP2	Define design space through DOE for critical method parameters.	MODS defined, system suitability mixture of impurities should be injected in every	3	1	1	3	89
Merging of DP3 & Main analyte		analysis and a minimum resolution of 1.2 set as criteria.	3	3	1	3	89
Merging of main analyte & DP4			3	3	1	3	89
LOQ of impurities	UPLC method preferred in place of HPLC. Method should be validated for accuracy, linearity, and precision at LOQ level	UPLC method developed, validated, and proven to be accurate, precise and linear at LOQ concentration.	2	2	1	4	77
Recovery	Method to be validated for accuracy	Method validated for recovery and found accurate. Recovery was found to be between 90.0% and 110.0% for Nintedanib	1	1	3	3	75

Table 15 Listing of Critical method and material attributes and their impact on CQAs.

% spike level	Amount added (% w/w)	% Recovery	Mean % recovery	% RSD	Precision (%RSD)			Range	Linearity	LOQ
	In triplicate				Injection	Inter-day	Intraday			
LOQ (0.0002 mg/mL)	0.0002 0.0002 0.0002	97.3 96.3 96.1	96.6	0.7	1.40%	2.60%	3.90%	0.0002 mg/mL to 0.004 mg/mL	Correlation Coefficient (r): 0.998	0.0002 mg/mL, Precision at LOQ: 4.5%RSD
50 (0.001 mg/mL)	0.001 0.001 0.001	100.1 101.3 103.2	101.5	1.5					Regression Coefficient (r^2): 0.996	
100 (0.002 mg/mL)	0.002 0.002 0.002	104.6 96.7 97.1	99.5	4.5					Slope: 23612867.38	
200 (0.004 mg/mL)	0.004 0.004 0.004	97.2 100.4 96.8	98.1	2					Intercept: −182.89, % Y-Intercept; 0.8%	

m/*z* 219 is evidence of ring opening at position 4 and thus N-oxide formation at position 4. These MS/MS data lead to the conclusion that NIN 4-N-oxide is 4-({[4-({[(3Z)-6-(methoxycarbonyl)-2-oxo-1H-indol-3-ylidene] (phenyl)methyl} amino) phenyl] (methyl) carbamoyl} methyl) -1-methylpiperazin-1-ium-1-olate.

The product ions at *m*/*z* 412 (loss of $C_6H_{12}N_2O_2$), *m*/*z* 399 (loss of CH from *m*/*z* 412), *m*/*z* 294 (loss of C_7H_9N from *m*/*z* 399), and *m*/*z* 209 (loss of methyl (3Z)-3-[amino(phenyl)methylidene]-2-oxo-1H-indole-6-carboxylate and piperazine ring opening at position 4) were observed in the ESI-MS/MS spectrum of *m*/*z* of 556 (DP4) (refer supplementary document).

Table 16 List of fragments observed in ESI/MS/MS.

Rt	Name	m/z $[M+H]^+$	ESI^+ MS/MS Fragments
0.97	DP1	263	151, 136, 113
1.13	DP2	526	398, 385, 249
2.04	DP3	556	412, 399, 294, 219
2.54	NIN	540	412, 398, 385, 294, 249
3.15	DP4	556	412, 399, 294, 209
8.61	DP5	296	219, 190

The fragment m/z 209 is evidence of ring opening at position 1 and thus N-oxide formation at position 1. These MS/MS data lead to the conclusion that NIN 1-N-oxide is 1-({[4-({[(3Z)-6-(methoxycarbonyl)-2-oxo-1H-indol-3-ylidene] (phenyl)methyl} amino) phenyl] (methyl) carbamoyl} methyl)-4-methylpipera zin-1-ium-1-olate.

3.9.6. Degradation mechanism

Under acid-mediated degradation, protonation followed by hydrolysis of the secondary amine resulted in DP1 (amine) and DP5 (alcohol), as depicted in Scheme 2. Under base-mediated degradation, NIN was hydrolyzed into DP2 by hydrolysis of the ester in the indole ring and methanol (Scheme 3). In the presence of hydrogen peroxide, oxidation of nitrogen atoms in the piperazine ring at positions 4 and 1 resulted in the formation of DP3 and DP4, respectively (Scheme 4).

Table 17 Calculated mass and observed m/z.

Proposed molecular formula $[M+H]^+$	Observed (m/z)	Calculated (Mol wt, $[M+H]^+$
$C_{31}H_{34}N_5O_4^+$	540	540.644
$C_{30}H_{32}N_5O_4^+$	526	526.617
$C_{17}H_{14}NO_4^+$	296	296.302
$C_{31}H_{34}N_5O_5^+$	556	556.643
$C_{31}H_{34}N_5O_5^+$	556	556.643
$C_{14}H_{22}N_4O^+$	263	263.365
$C_{25}H_{22}N_3O_3^+$	412	412.469
$C_{24}H_{21}N_3O_3^+$	399	399.450
$C_{24}H_{20}N_3O_3^+$	398	398.450
$C_{23}H_{19}N_3O_3^+$	385	385.423
$C_{17}H_{14}N_2O_3^+$	294	294.310
$C_{14}H_{23}N3_O^+$	249	282.299
$C_{11}H_{17}N_3O^+$	219	249.358
$C_{11}H_{17}N_3O^+$	207	219.288
$C_{10}H_8NO_3^+$	190	141.194
$C_8H_{10}N_2O^+$	151	151.189
$C_8H_{12}N_2^+$	136	136.198
$C_6H_{14}N_2^+$	113	113.184

4. Conclusion

In view of the limited information and guidelines on analytical QbD, a stepwise and systematic procedure for implementing QbD in analytical method development is methodically formulated in this article. A

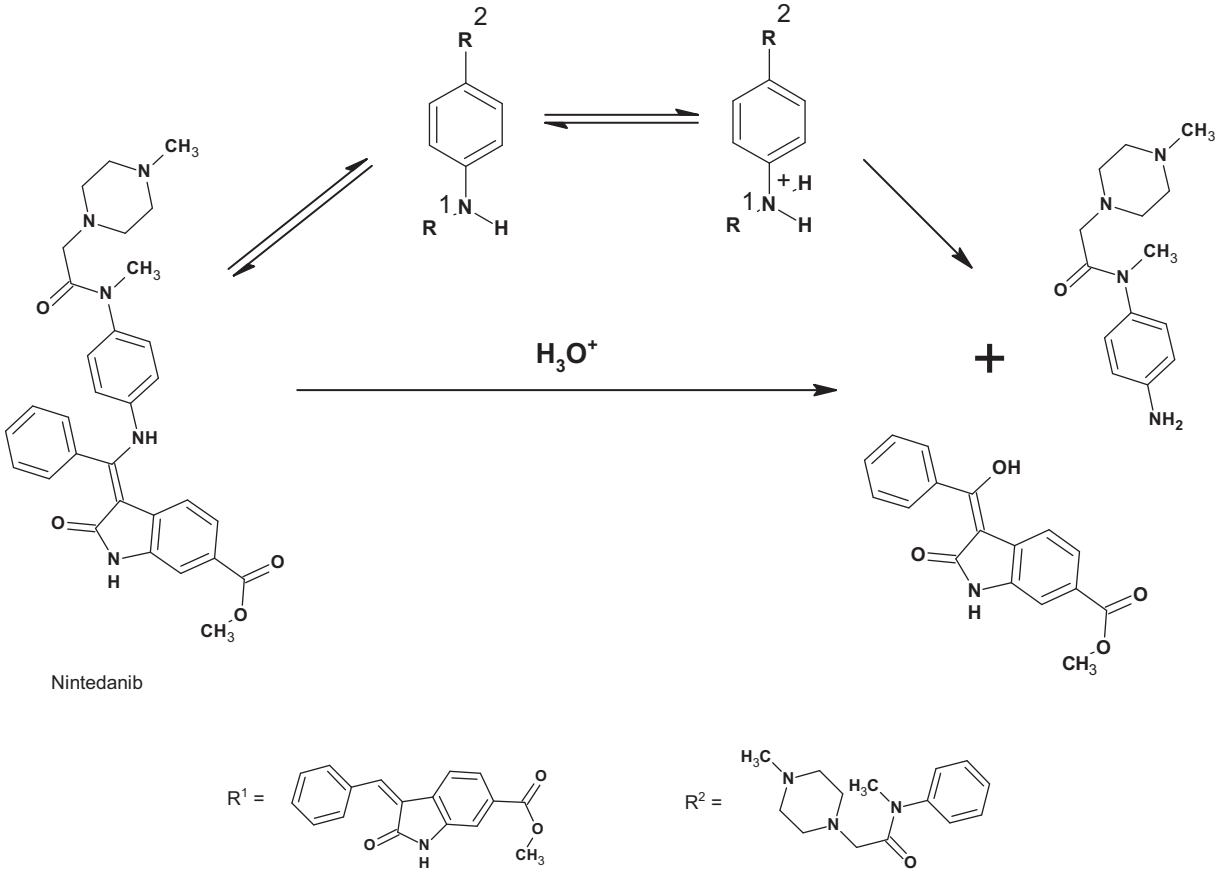

Scheme 2 Proposed Acid hydrolysis reaction mechanism.

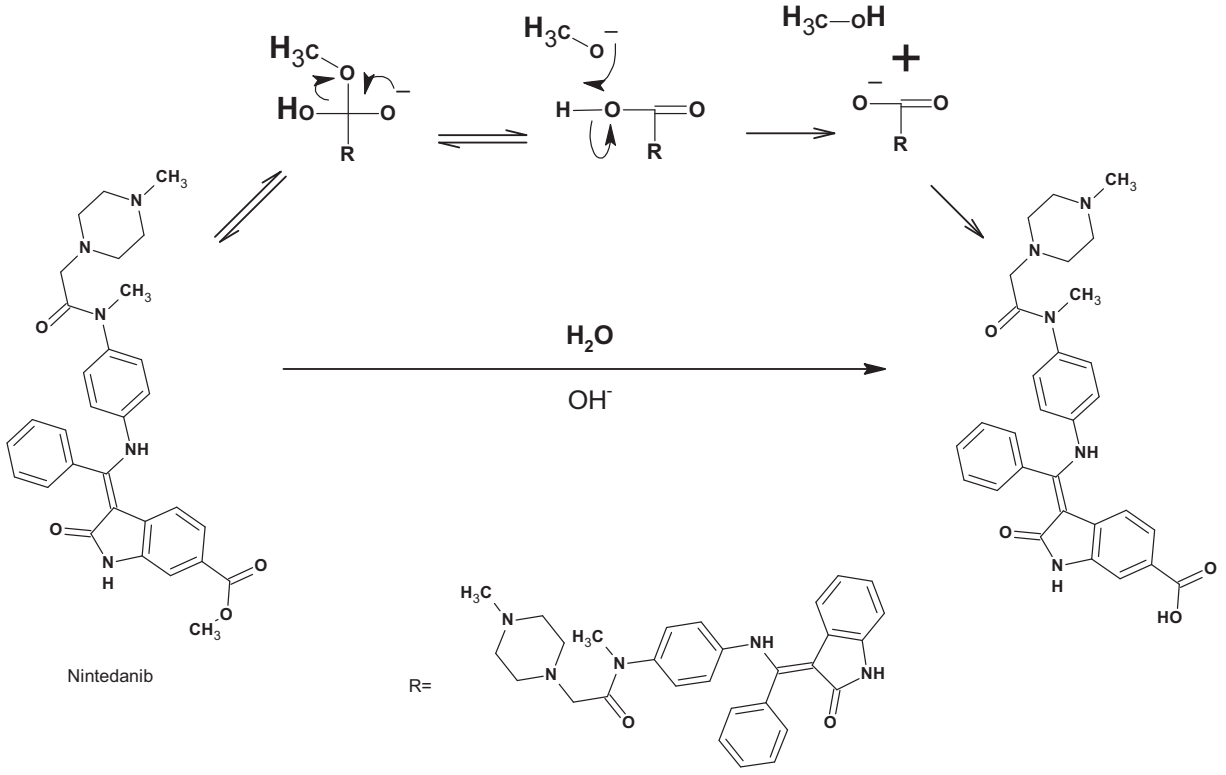

Scheme 3 Proposed base hydrolytic reaction mechanism.

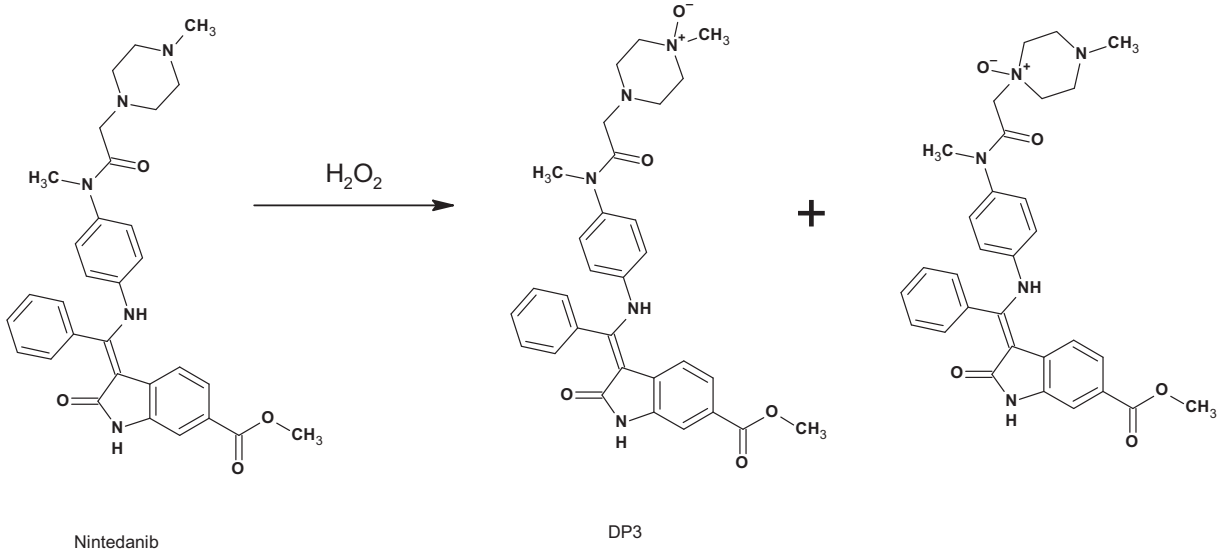

Scheme 4 Proposed oxidative reaction mechanism.

simple and novel experimental test method for estimating products derived from the degradation of NIN soft gelatin capsules is successfully developed using a UPLC technique with a shorter run time of 12 min. Further, for the first time it is applied to an FMEA-based risk assessment for the analytical method development of NIN. A detailed statistical analysis and design space are established through DOE for the developed method. Incidentally, the method is proved to be robust for wider conditions of variation. Control strategies are well defined to reduce the potential risk and improve the detectability of sample concentration. Important information on the possible chemical vulnerability and sensitivity of the test molecule to hydrolytic and oxidative exposure is made available through the proposed degradation pathway. This information supports and guides the formulators to design and develop proper formulated products by selecting suitable excipients and process and packaging methods. Five major degradation products are separated via chromatographic methods and character-

ized using MS/MS. This approach provides a detailed protocol for the formulators to monitor and characterize the potential impurities during the stability testing under scientifically acceptable specified threshold limits and within the qualifiable level as per ICH Q3 guidelines.

Declaration of Competing Interest

The authors declare that they have no known competing financial interests or personal relationships that could have appeared to influence the work reported in this paper.

Appendix A. Supplementary material

Supplementary data to this article can be found online at https://doi.org/10.1016/j.arabjc.2020.07.014.

References

Abboud, L., Hensley, S., 2003. New prescription for drug makers: Update the plants. Wall Str. J. 3–9. https://www.wsj.com/articles/SB10625358403931000 (accessed June 2, 2019).

Agency, E.M., 2011. European Medicines Agency: An unacceptable choice. Prescrire Int. 20, 278.

Basso, J., Mendes, M., Cova, T.F.G.G., Sousa, J.J., Pais, A.A.C.C., Vitorino, C., 2018. Analytical Quality by Design (AQbD) as a multiaddressable platform for co-encapsulating drug assays. Anal. Meth. 10, 5659–5671. https://doi.org/10.1039/c8ay01695j.

Beg, S., Sharma, G., Katare, O.P., Lohan, S., Singh, B., 2015. Development and Validation of a Stability-Indicating Liquid Chromatographic Method for Estimating Olmesartan Medoxomil Using Quality by Design, pp. 1–12.

Beg, S., Chaudhary, V., Sharma, G., Garg, B., 2016. QbD-oriented development and validation of a bioanalytical method for nevirapine with enhanced liquid – liquid extraction and chromatographic separation, pp. 818–828. https://doi.org/10.1002/bmc.3613.

Dasari, P., Arava, V., Life, S., Limited, S., Gogireddy, S.R., Life, S., Limited, S., Bethi, M.R., Life, S., Limited, S., Development, A.M., 2015. Development and validation of a simple and sensitive stability indicating RP-HPLC assay method for determination of Nintedanib and stress degradation studies Development and validation of a simple and sensitive stability indicating RP-HPLC assay method fo.

Devrukhakar, P.S., Shiva Shankar, M., Shankar, G., Srinivas, R., 2017. A stability-indicating LC–MS/MS method for zidovudine: Identification, characterization and toxicity prediction of two major acid degradation products. J. Pharm. Anal. 7, 231–236. https://doi.org/10.1016/j.jpha.2017.01.006.

Devrukhakar, P.S., Shankar, G., Srinivas, R., 2018. Proposal of degradation pathway with toxicity prediction for hydrolytic and photolytic degradation products of timolol. J. Pharm. Biomed. Anal. 154, 7–15. https://doi.org/10.1016/j.jpba.2018.02.057.

Görög, S., Baertschi, S.W., 2013. The role of analytical chemistry in drug-stability studies. TrAC Trends Anal. Chem. 49, 55–56. https://doi.org/10.1016/j.trac.2013.06.001.

Hutchinson, J., Fogarty, A., Hubbard, R., McKeever, T., 2015. Global incidence and mortality of idiopathic pulmonary fibrosis: A systematic review. Eur. Respir. J. 46, 795–806. https://doi.org/10.1183/09031936.00185114.

ICH HARMONISED TRIPARTITE GUIDELINE, 2004, In: Pharm. Dev. Q8. ICH, Geneva. https://www.ich.org/fileadmin/Public_Web_Site/ICH_Products/Guidelines/Quality/Q8_R1/Step4/Q8_R2_Guideline.pdf.

ICH, 1998. Q1B Photostability Testing of New Active Substances and Medicinal Products. Eur. Med. Agency, pp. 1–9. http://www.ema.europa.eu/docs/en_GB/document_library/Scientific_guideline/2009/09/WC500002647.pdf.

Jayagopal, B., Shivashankar, M., 2017. Analytical Quality by Design – A Legitimate Paradigm for Pharmaceutical Analytical Method Development and Validation. Mech. Mater. Sci. Eng. J. 9, 10. https://doi.org/10.2412/mmse.96.97.276.

Juran, J.M., Godfrey, A.B., 1998. Juran's Quality Control Handbook. https://doi.org/10.1108/09684879310045286.

Karmarkar, S., Garber, R., Genchanok, Y., George, S., Yang, X., Hammond, R., 2011. Quality by design (QbD) based development of a stability indicating HPLC method for drug and impurities. J. Chromatogr. Sci. 49, 439–446. https://doi.org/10.1093/chrsci/49.6.439.

Keating, G.M., 2015. Nintedanib: A Review of Its Use in Patients with Idiopathic Pulmonary Fibrosis. Drugs 75, 1131–1140. https://doi.org/10.1007/s40265-015-0418-6.

Khalique, S., Banerjee, S., 2017. Nintedanib in ovarian cancer. Expert Opin. Investig. Drugs. 26, 1073–1081. https://doi.org/10.1080/13543784.2017.1353599.

Kochling, J., Wu, W., Hua, Y., Guan, Q., Castaneda-Merced, J., 2016. A platform analytical quality by design (AQbD) approach for multiple UHPLC-UV and UHPLC-MS methods development for protein analysis. J. Pharm. Biomed. Anal. 125, 130–139. https://doi.org/10.1016/j.jpba.2016.03.031.

Mazzei, M.E., Richeldi, L., Collard, H.R., 2015. Nintedanib in the treatment of idiopathic pulmonary fibrosis, 121–129. https://doi.org/10.1177/1753465815579365.

Mohammed, A.Q., Sunkari, P.K., Mohammed, B., Srinivas, P., Roy, A.K., 2015. Quality by Design (QbD) in Action-2 : Controlling Critical Material Attributes (CMA) during the synthesis of an API.

Plumb, R., Castro-Perez, J., Granger, J., Beattie, I., Joncour, K., Wright, A., 2004. Ultra-performance liquid chromatography coupled to quadrupole-orthogonal time-of-flight mass spectrometry. Rapid Commun. Mass Spectrom. 18, 2331–2337. https://doi.org/10.1002/rcm.1627.

Smith, K.M., 2018. Analysis of Pharmaceutical Drugs Using the ACQUITY UPLC I-Class PLUS System and the Xevo TQ-S Mass Spectrometer, Waters Technol. Br. 1–3. https://www.waters.com/waters/library.htm?locale=en_US&lid=134976284&cid=511436.

Taylor, P., Garg, N.K., Sharma, G., Singh, B., Nirbhavane, P., Prakash, O., 2015. Journal of Liquid Chromatography & Related Quality by Design (QbD) -based Development and Optimization of a Simple, Robust RP HPLC Method for the Estimation of Methotrexate. https://doi.org/10.1080/10826076.2015.1087409.

Tepede, A., Yogaratnam, D., 2017. Nintedanib for Idiopathic Pulmonary Fibrosis. J. Pharm. Pract. https://doi.org/10.1177/0897190017735242.

Togami, K., Fukuda, K., Yamaguchi, K., Chono, S., Tada, H., 2018. Facile and sensitive HPLC-UV method for determination of nintedanib in rat plasma, 10.

Yadav, N.K., Raghuvanshi, A., Sharma, G., Beg, S., Katare, O.P., Nanda, S., 2015. QbD-Based Development and Validation of a Stability-Indicating HPLC Method for Estimating Ketoprofen in Bulk Drug and Proniosomal Vesicular System, pp. 1–13. https://doi.org/10.1093/chromsci/bmv151.

5.1.7. https://www.drugbank.ca/drugs/DB09079. 2020. (Accessed 02 March 2020).